European Journal of Pharmaceutics and Biopharmaceutics 178 (2022) 168–178

Contents lists available at ScienceDirect

European Journal of Pharmaceutics and Biopharmaceutics

journal homepage: www.elsevier.com/locate/ejpb

Research paper

Modelling drug diffusion through unstirred water layers allows real-time quantification of free/loaded drug fractions and release kinetics from colloidal-based formulations

Martina M. Tzanova [a,1], Federica Moretti [b,1], Gabriele Grassi [c], Paul C. Stein [d], Marianne Hiorth [a], Michela Abrami [b], Mario Grassi [b], Massimiliano Pio di Cagno [a,*]

[a] Department of Pharmacy, Faculty of Mathematics and Natural Sciences, University of Oslo, Sem Saelands vei 3, 0371 Oslo, Norway
[b] Department of Engineering and Architecture, University of Trieste, Via Alfonso Valerio, 6/1, 34127 Trieste, Italy
[c] Department of Medicine, Surgery and Health Sciences, Strada di Fiume 447, 34149 Trieste, Italy
[d] Department of Physics, Chemistry and Pharmacy, University of Southern Denmark, 5230 Odense, Denmark

ARTICLE INFO

Keywords:
Cyclodextrins
Liposomes
Drug diffusion
Molecularly dissolved drug
Mathematical modelling
Numerical data fitting

ABSTRACT

The correlation between *in vivo* and *in vitro* data is yet not sufficiently optimized to allow a significant reduction and replacement of animal testing in pharmaceutical development. One of the main reasons for this lies in the poor mechanistic understanding and interpretation of the physical mechanisms enabling formulation rely on for deploying the drug. One mechanism that still lacks a proper interpretation is the kinetics of drug release from nanocarriers. In this work, we investigate two different types of classical enabling formulations – i) cyclodextrin solutions and ii) liposomal dispersions – by a combination of an experimental method (i.e. UV–Vis localized spectroscopy) and mathematical modelling/numerical data fitting. With this approach, we are able to discriminate precisely between the amount of drug bound to nanocarriers or freely dissolved at any time point; in addition, we can precisely estimate the binding and diffusivity constants of all chemical species (free drug/bound drug). The results obtained should serve as the first milestone for the further development of reliable *in vitro/in silico* models for the prediction of *in vivo* drug bioavailability when enabling formulations are used.

1. Introduction

Liposomes and cyclodextrins are two of the most investigated drug carriers of the last century. Liposomes are spherical phospholipid bilayers that are capable of carrying both hydrophilic (in the aqueous core) and lipophilic (in the lipid bilayer) compounds [1]. In the last years, several liposomal formulations have reached the market and are currently used in the treatment of various diseases from fungal infections (e.g. amphotericin B liposomal dispersion, brand name Amphotec®/Ambisome®) to cancer (e.g. doxorubicin-liposome dispersions, brand name Myocet® or Daunorubicin-liposomes product name Vyxeos®) [2].

On the other hand, cyclodextrins (CD) (Fig. 1) have been heavily investigated as solubilizing agents especially for poorly water-soluble compounds. Cyclodextrins are cyclic oligosaccharides, among which the most common are composed of 6 (α-CD), 7 (β-CD) and 8 (γ-CD) glucose units [3]. The distinct trunked-cone shape and the very hydrophilic outer surface area allow lipophilic moieties (e.g. aromatic rings, short aliphatic chains) to be spontaneously incorporated into the CD lipophilic core of the dextrin ring, forming a complex. For pharmaceutical purposes, the most employed cyclodextrin is the β-type and its hydrophilic derivatives (e.g. 2-hydroxypropyl-β-CD, Fig. 1). Despite its hydrophilicity, the standard β-CD suffers from poor aqueous solubility due to a strong intramolecular network of H-bonds. Water-soluble derivatives such as 2-hydroxypropyl-β-cyclodextrin (HP-β-CD) and sulfobutylether-β-cyclodextrin (SBE-β-CD) are GRAS approved and widely used in food and drug industries as excipients [4]. Nowadays, several cyclodextrins-based pharmaceutical formulations are available on the market e.g. the branded drug Veklury®, the first anti-retroviral drug approved for the treatment of SARS-CoV-2 infection, is an aqueous solution of SBE-β-CD-remdesivir complex with molar ratio 16:1 [5].

Eq. (1) describes the most general equilibrium between a ligand (e.g.

* Corresponding author.
E-mail address: m.p.d.cagno@farmasi.uio.no (M.P. di Cagno).
[1] These authors contributed equally to this work.

https://doi.org/10.1016/j.ejpb.2022.08.009
Received 3 June 2022; Received in revised form 27 July 2022; Accepted 20 August 2022
Available online 25 August 2022

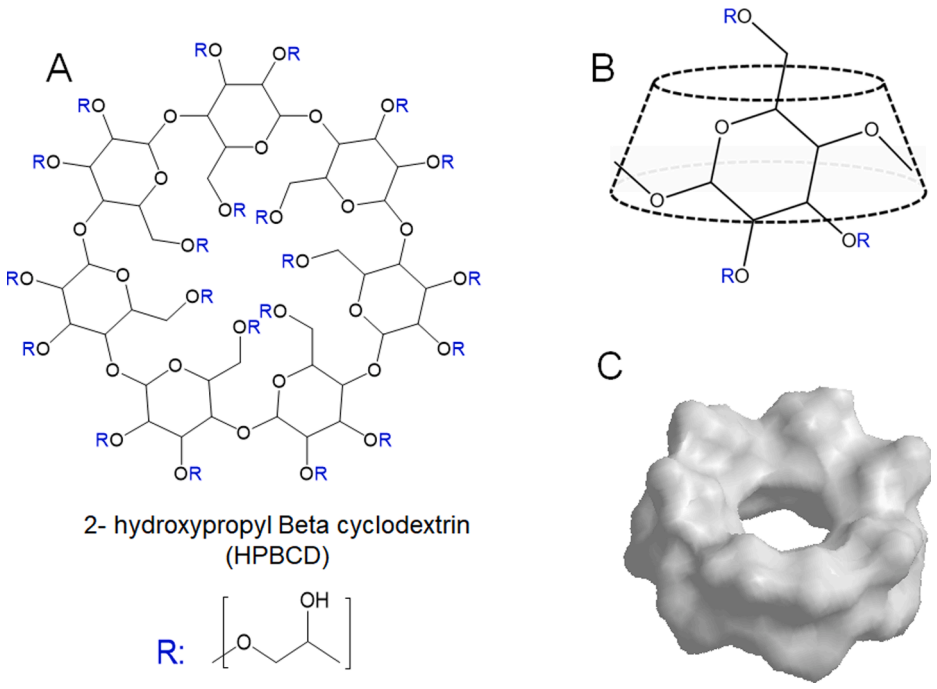

Fig. 1. Chemical structure of β-cyclodextrin (β-CD, R:-H) and the derivative used in this study 2-hydroxypropyl-β-cyclodextrin (HP-β-CD). The figure also shows the classical trunked-cone structure of the native compound (B) as well as its three-dimensional conformation (C) in aqueous environment.

cyclodextrin, liposomes) and a substrate (e.g. a drug molecule):

$$nL + mS \leftrightarrow L_n - S_m \tag{1}$$

where L and S represent the ligand and substrate, respectively, (with the respective stoichiometric factors n and m) and L_n-S_m is the complex formed. The most general equilibrium constant (K_{eq}) for this equilibrium can be written as Eq. (2):

$$K_{eq} = \frac{[L_n - S_m]}{[L]^n * [S]^m} \tag{2}$$

where [L_n-S_m] represents the concentration of the complex at equilibrium and [L] and [S] represent the free drug fraction and the ligand free fraction concentrations at equilibrium (each concentration raised to its stoichiometric factor). The efficiency of this carrier-based solubilizing agent in enhancing biopharmaceutical performances *in vivo,* especially of poorly water-soluble drugs, remains a big question mark. In fact, even though both liposomes and CDs are capable of solubilizing poorly soluble substances [6,7] by enhancing their apparent solubility in water by several orders of magnitude, in some cases absorptions rate of these drugs *in vitro* [8] and *in vivo* are unmodified or even reduced [9–11]. One accredited hypothesis to explain these phenomena is the *free-drug-fraction* paradox that limits the absorption of BCS (Biopharmaceutics Classification System) class II and IV (low solubility) drugs through biological barriers with solubilizers [12]. According to Fick's first law of diffusion (Eq. (3)), the flux (j) through a barrier (e.g. GI tract) should be proportional to the drug diffusivity constant (D) in the diffusion media and the concentration gradient (dc/dx):

$$j = -D\frac{dc}{dx} \tag{3}$$

Assuming that the concentration gradient (dc/dx) is constant, Eq. (3) can be written as:

$$j = \overline{D}\frac{c_d - c_a}{h} \tag{4}$$

where c_d and c_a are the concentrations of the drug in the donor and acceptor compartment respectively, h is the barrier thickness and $\overline{D}$ is the average diffusivity of the drug in the donor/acceptor media (basically water) and in the barrier (lipoidal environment). The free-drug-fraction paradox refers to the fact that, when carrier-based enabling formulations are employed (e.g. liposomes, micelles), the decisive parameter determining drug permeation and absorption is mostly, if not only, the free drug concentration (i.e. the molecularly dissolved drug, [S]) [12]. Therefore, Eq. (4) can be written as:

$$j = \overline{D}\frac{[S]}{h} \tag{5}$$

We have demonstrated the validity of this phenomenon for liposomal and micellar dispersions loaded with hydrocortisone and utilized sheep nasal mucosa as the barrier of absorption [13]. In order to further extend our comprehension of the free-drug-fraction paradox – that is the key to improve the *in silico* predictability of enabling formulation systems – there is an urgent need for a method able to reliably measure real time the free drug concentration ([S]) and the bound drug concentration ([L_n-S_m], Eq. (3)). So far, few empirical methods are available for the estimation of free-drug fraction (i.e. molecularly dissolved drug) from nanocarriers. For larger drug carriers such as liposomes and micelles, the most employed are dialysis, centrifugation, size exclusion chromatography [14] and microdialysis/nanofiltration [15]. These methods are quite impractical as they all require dedicated laboratory apparatus and, additionally, they induce perturbation of the equilibrium system. For cyclodextrins, the free-drug fraction can be estimated by phase-solubility studies or by isothermal titration calorimetry (ITC) [7]. Yet again, ITC is a quite uncommon equipment in pharmaceutical laboratories and experiments are not easy to perform. An empirical/computational method based on localized UV–Vis spectroscopy for studying the passive diffusion of drugs in unstirred layers has earlier been introduced by us [16]. We showed that through fitting a simple analytical solution of Fick's second law of diffusion to the empirical diffusion curves, it is possible to obtain precise diffusivity parameters for drugs in solution, as well as in formulations. Unfortunately, the mathematical approach utilized previously proved to be insufficient for precisely quantify the equilibrium constant drug-liposomes, as well as to give a precise estimation of the free drug fraction, [S], in liposomal dispersions and cyclodextrin solutions [17]. The aim of this work was to

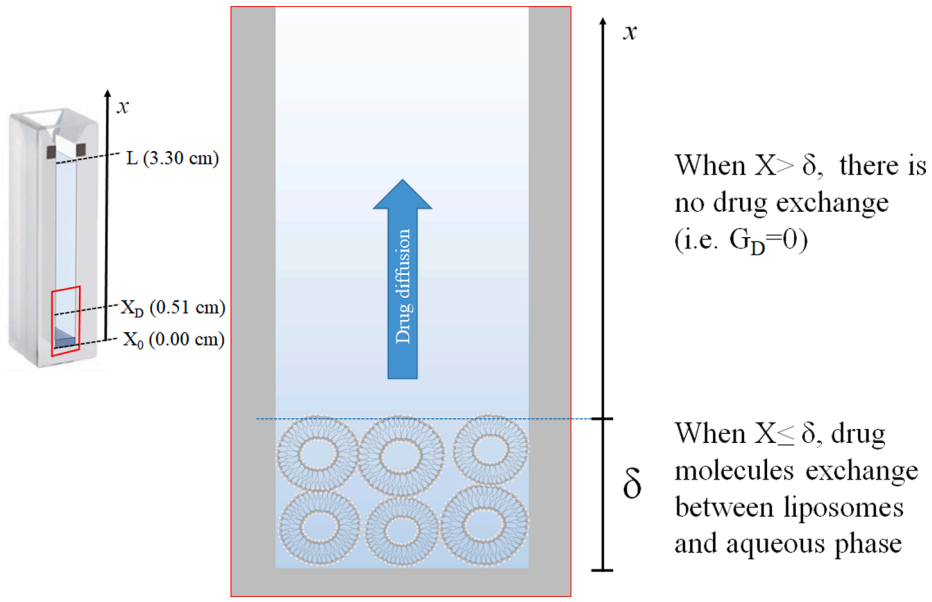

Fig. 2. Schematic representation of the diffusional system recreated inside a UV–vis standard quartz cuvette.

use localized UV–Vis spectroscopy to study the diffusion of drugs in the presence of HP-β-CD and liposomes and utilize an extended mathematical approach to interpret the empirical diffusion data. This new approach allows the simultaneous and real time measurement of several relevant parameters such as the free drug concentration [*S*] the bounded drug concentration [S_n-L_m] as well as the equilibrium constants (K_{eq}), opening the gate to *in silico* permeation prediction of such formulations.

2. Experimental section

2.1. Materials

Hydrocortisone (HC), (2-hydroxypropyl)-β-cyclodextrin (HP-β-CD; DS = 0.5–1.3), ibuprofen (IBU) and sodium hydroxide (≥98.0% pellets; NaOH) were purchased from Sigma-Aldrich Chemie GmbH (Steinheim, DE). Acetonitrile (≥99.9% isocratic grade for HPLC; ACN), ethanol (96 % (v/v)) sodium chloride (NaCl) and sodium dihydrogen phosphate dihydrate ($NaH_2PO_4{\cdot}2H_2O$) were purchased from VWR Chemicals (Radnor, PA, USA). Chloroform (for analysis EMSURE®) and disodium phosphate dihydrate ($Na_2HPO_4{\cdot}2H_2O$) were purchased from Merck KGaA (Darmstadt, DE). Lipoid S100 (soybean phosphatidylcholine, ≥ 94 % pure; sPC) was a generous gift from Lipoid GmbH (Ludwigshafen, DE). All solutions and HPLC mobile phase were prepared with water, purified by a Milli-Q® water purification system for ultrapure water by Merck Millipore (Darmstadt, DE).

2.2. Solutions

Phosphate-buffered saline (PBS; 73 mM) with pH 7.4 was prepared by mixing one part 2.5% (w/v) $NaH_2PO_4{\cdot}2H_2O$ solution with four parts 0.9% (w/v) $Na_2HPO_4{\cdot}2H_2O$ solution. The pH was adjusted to 7.4 ± 0.05 (SevenCompact™ pH/ion meter S220; Mettler Toledo, Columbus, OH, USA) with NaOH pellets and osmolality – to 280–300 mOsm/kg (Semi-Micro Osmometer K-7400, Knauer, Berlin, DE) with NaCl. PBS was filtered 0.2 μm (Whatman® Nuclepore Track-Etch membrane filter; GE Healthcare Life Sciences, Maidstone, UK) prior to use.

2.3. Preparation of cyclodextrin solutions and post-loaded liposomal dispersions

Detailed samples preparation is presented by di Cagno and Stein [17]. Briefly, ibuprofen stock solution in PBS was mixed with increasing amounts of a HP-β-CD solution in PBS and the volume was adjusted adequately with the same solvent, yielding solutions with API concentration of 0.268 mg/cm^3 (=1.3 mM) and the following HP-β-CD concentrations: 0.698, 1.396, 3.940, 6.980 and 13.960 mg/cm^3 (=0.5, 1, 2.5, 5 and 10 mM, respectively). Additionally, the liposomal dispersion was prepared by the classical thin-film hydration method [18], dissolving SPC in methanol, evaporating the solvent and rehydrating the lipid film with PBS for a final lipid concentration of 40 mg/cm^3. The liposomes were extruded through 800 and 400 nm polycarbonate filters (4 cycles each) to obtain homogeneously dispersed vesicles of approximately 400 nm. The dispersion was subsequently mixed (1:1) and incubated for 10 min with a solution of hydrocortisone in PBS, yielding a dispersion with a final API concentration of 0.181 mg/cm^3. Since the loading of the liposomes took place after preparation, we choose to call these *post-loaded* liposomes, in contrast to the *pre-loaded* liposomes, described in the next section.

2.4. Preparation and basic characterization of pre-loaded liposomal dispersions

Liposomes were prepared by the classical thin-film hydration method. Initially, 500 mg sPC and 5 mg hydrocortisone were dissolved in 20 mL chloroform in a round-bottom flask (1 L). The organic solvent was evaporated at 40 °C for approximately 30 min using a rotary evaporator (Heidolph Hei-VAP Advantage, Schwabach, DE), followed by a one-hour freeze-drying (Christ Alpha 2–4 LSCplus Martin Christ Gefriertrocknungsanlagen GbmH, Osterode am Harz, DE), in order to remove solvent rests. The lipid film was subsequently reconstituted with 10 mL PBS and left at room temperature overnight, prior the extrusion. The size of the liposomes was reduced by a stepwise extrusion through two stacked polycarbonate membranes (25 mm Nuclepore™ Track-Etch Membrane, Whatman®, Maidstone, UK) of descending pore sizes – 800 nm (10 cycles) and 400 nm (20 cycles) – at room temperature in a 10 mL Lipex® extruder (Lipex Biomembranes Inc., Vancouver, CA). The liposomes were characterized immediately after extrusion and used in the diffusion measurements, as described in section 2.5. For the particle size determination, the intensity-mean hydrodynamic diameter (z-average (nm)) and particle size distribution (polydispersity index (PdI) were measured using dynamic light scattering (DLS) with a red light laser (λ = 633 nm) at 25 °C by Zetasizer Nano-ZS (Malvern Instruments, Oxford,

UK). The refractive index and the viscosity of pure water at 25 °C were used as constant parameters in the calculations. The analysis (300 s, 3 cycles, 25 °C) was performed on a liposomal sample diluted 1:800 with PBS in disposable polystyrene cuvette for Zetasizer (Sarstedt AG & Co., Nümbrecht, DE). For determining the final concentration of hydrocortisone in the liposomal dispersion, an aliquot was diluted 1:100 in ethanol (in order to destroy the phospholipid vesicles and release the API) and subsequently diluted 1:1 with Milli-Q® prior to quantification with high-performance liquid chromatography (HPLC). The analysis was performed on an UltiMate 3000RS system (Thermo Scientific™ Dionex™, Sunnyvale, CA, USA), equipped with a Nova-Pak C18 guard column (3.9 × 20 mm) and analytical column (3.9 × 150 mm, 60 Å, 4 μm; Waters™, Milford, MA, USA) and UV detector (at 254 nm). Mobile phase consisted of ACN and Milli-Q® water and separation was achieved by a 4-minutes linear gradient from 5 to 95 % ACN at a flow rate of 1 mL/min. Column oven temperature was set to 30 °C, the retention time was 4.6 min and the total run time was 12 min. The injection volume was 80 μL and two injections per vial were analysed. Standard solutions (concentration range: 1–10 μg/cm^3; $R^2 \geq 0.999$) were analysed in a similar manner at the beginning and the end of the sequence, to ensure system changes were detected and could be accounted for.

2.5. Diffusion

Localized UV–Vis spectroscopy measurements were performed on a double array UV–Vis spectrophotometer UV-6300PC (VWR International, Radnor, PA, USA) in semi-micro cuvettes with PTFE stopper ($V_{chamber}$ = 700 μL, path length = 10 mm; Starna Scientific®, Essex, UK), as described previously [16]. The diffusion medium and reference sample (675 μL each) consisted of Milli-Q®, whilst the donor solution contained one of the three formulations: a solution of HP-β-CD and ibuprofen or one of the liposomal dispersions post- or pre-loaded with hydrocortisone. At time zero (t = 0 s), donor solution (25 μL) was injected at the bottom of the sample cuvette using a microneedle syringe (Hamilton Company, Reno, NV, USA). Absorbance measurements were recorded at 221 and 248 nm for ibuprofen and hydrocortisone, respectively, every 120 s for a total of 24 h. For all experiments, the sample cuvette was lifted by 0.60 cm using a 3D-printed stand, in order to record absorbances at precisely 0.51 cm (detection position, X_D, see Fig. 2) from the bottom of the cuvette (i.e. the origin of diffusion), as previously detailed by Di Cagno *et al.* [16]. For cyclodextrins and post-loaded liposomes, we utilized raw diffusion data set previously acquired [17]. All measurements were performed once.

3. Mathematical model

The mathematical model presented is based on the species mass balance embodying Fick's law of diffusion and accounting for a generative term (G_i) [19]:

$$\frac{\partial C_i(x,t)}{\partial t} = D_i \frac{\partial^2 C_i(x,t)}{\partial x^2} + G_i \tag{6}$$

where C_i represents the concentration of the ith diffusing species [mass/volume], D_i is the ith species diffusion coefficient [squared length/time] (assumed constant in time and space for all the diffusing species), t is the time and x is the diffusion path (assuming the diffusion to be significant only in one direction, i.e. the height of the cuvette; cm). The generative term G_i [mass/volume time] assumes different expressions depending on the possible interactions among diffusing species (cyclodextrins case) or on mass exchange between phases (liposomes case).

3.1. Cyclodextrins

The interaction between drug (D) and cyclodextrin (C), (Eq. (1)) can be written as:

$$mD + nC \underset{k_2}{\overset{k_1}{\rightleftarrows}} DC \tag{7}$$

where D, C and DC are the free drug, free cyclodextrin and complex molar concentrations, respectively, k_1 and k_2 are the binding and unbinding kinetic constants, respectively, while m and n are the chemical reaction stoichiometric coefficients. According to Eq. (7), it is possible to evaluate the generative terms relative to drug (G_D), cyclodextrin (G_C) and drug-cyclodextrin complex (G_{DC}) so that eq. (6) can be solved for each species as:

$$\frac{\partial C_D}{\partial t} = D_D \frac{\partial^2 C_D}{\partial x^2} + G_D G_D = M_D \left(m^* k_2^* C_{DC} - m^* k_1^* C_D^m * C_C^n \right) \tag{8}$$

$$\frac{\partial C_C}{\partial t} = D_C \frac{\partial^2 C_C}{\partial x^2} + G_C G_C = M_C \left(n^* k_2^* C_{DC} - n^* k_1^* C_D^m * C_C^n \right) \tag{9}$$

$$\frac{\partial C_{DC}}{\partial t} = D_{DC} \frac{\partial^2 C_{DC}}{\partial x^2} + G_{DC} G_{DC} = M_{DC} \left(k_1^* C_D^m * C_C^n - k_2^* C_{DC} \right) \tag{10}$$

where C_D, C_C and C_{DC} are the drug, cyclodextrin and drug-cyclodextrin complex concentrations [mass/volume], respectively, while D_D, D_C and D_{DC} and M_D, M_C and M_{DC} are, respectively, the diffusion coefficients [length^2/time] and molar weights of the three respective chemical species involved.

The boundary conditions referring to Eqs. (8)–(10) imply an impermeable wall in $X = X_0$ (bottom of the cuvette, Fig. 2) and $X = L$ (full cuvette length) directions:

$$\left.\frac{\partial C_i}{\partial x}\right|_{X=0} = \left.\frac{\partial C_i}{\partial x}\right|_{X=L} = 0 \quad \forall i(D, C, DC) \tag{11}$$

Initial conditions assume that the drug is absent in the cuvette (C_D = 0) except for its initial part ($X \leq \delta \approx 1200$ μm) where the injected solution volume resides. Thus, for $X \leq \delta$, it is assumed that the initial drug, HP-β-CD and complex concentrations are uniform and attain the thermodynamic equilibrium evaluable by the solution of the following equations:

$$C_{DCE} = \frac{k_1}{k_2} * C_{DE}^m * C_{CE}^n \tag{12}$$

$$\left(C_{DE} + C_{DCE} m \frac{M_D}{M_{DC}} \right) V_s = C_{D0} V_s \tag{13}$$

$$\left(C_{CE} + C_{DCE} n \frac{M_C}{M_{DC}} \right) V_s = C_{C0} V_s \tag{14}$$

where V_s represents the injected volume [length^3], C_{D0} and C_{C0} are the drug and cyclodextrin concentrations used to prepare the injected solution, while C_{DE}, C_{CE}, and C_{DCE} are the drug, cyclodextrin and complex equilibrium concentrations (i.e. the initial concentration values in the injected volume), respectively. While Eq. (12) corresponds to the attainment of equilibrium among drug, cyclodextrin and complex concentrations, Eqs. (13) and (14) are the mass balance referring to drug and cyclodextrin in the injected volume. The iterative numerical solution (implicit Euler method, tolerance 10^{-8}) of Eqs. (12)–(14) allows the determination of C_{DE}, C_{CE}, and C_{DCE} (see details in Supporting Information).

Time and special discretization of Eqs. (8)–(10) was performed according to the control volume method [20], while the resulting nonlinear system of algebraic equations was iteratively solved by means of the Gauss-Seidel method embodying a relaxation step (relative tolerance 10^{-8}) [21]. In order to ensure the numerical solution stability and accuracy, the time discretization step was set to 1 s while the space discretization step was set to 60 μm (1/500th of the total cuvette length). The numerical solution was achieved by means of a proper Fortran

program.

3.2. Liposomes

The drug diffusion phenomenon in presence of liposomes in an unstirred aqueous phase requires accounting for the drug exchange occurring between the aqueous phase and the liposomes and this can be modelled by a proper definition of the generative term (Eq. (6)). In this work, we assume that the drug exchange between the two phases can be described as a drug partitioning between two immiscible phases [22]:

$$G_D = \left(k_1 * C_{lip} \left(\frac{C_{DS} - C_D}{C_{DS}} \right) - k_2 * C_D \left(\frac{C_{lipS} - C_{lip}}{C_{lipS}} \right) \right) \quad (15)$$

where C_D and C_{lip} are the drug concentrations in the aqueous and liposomal phases, respectively, C_{DS} and C_{lipS} are the drug solubility in the aqueous and the liposomal phases [mass/volume], respectively, while k_1 and k_2 are two kinetic constants [dimension length/time]. With this mathematical interpretation, drug release from the liposomes to the aqueous phase can occur on condition that $C_{lip} \neq 0$ and that the drug concentration in the aqueous phase (C_D) is lower than the solubility threshold (C_{DS}). Similarly, the drug loading (i.e. transport of drug from the aqueous phase into liposomes) can occur on condition that $C_D \neq 0$ and that the drug concentration in the liposomal phase (C_{lip}) is lower than the solubility threshold (C_{lipS}). Eq. (15) represents a generalization of the approach proposed by Van de Waterbeemd and co-workers [23] that applies only for soluble drugs in both the hydrophilic and hydrophobic phases, i.e. in the limit $C_D/C_{DS} \approx 0$ and $C_{lip}/C_{lipS} \approx 0$. The volume fractions of the injected volume occupied by liposomes and aqueous phase are φ_p (a known parameter) and (1-φ_p), respectively. In addition, due to the presence of liposomes, the cuvette cross-section available for drug diffusion will be lower than the geometrical value. Thus, assuming monodisperse size distribution of the liposomes, the available cross section turns out to be equal to (1–1.5* φ_p) [24]. Taking all this into account, eq. (6) can be re-written as:

$$\frac{\partial C_D}{\partial t} = \left(\frac{1 - 1.5\varphi_p}{1 - \varphi_p} \right) * D_D \frac{\partial^2 C_D}{\partial x^2} + \frac{3}{R_{lip}} * \left(\frac{\varphi_p}{1 - \varphi_p} \right) * G_D \quad X \leq \delta \quad (16)$$

where R_{lip} indicates the liposomes average radius while $3\varphi_p/R_{\mathrm{lip}}$ is the liposomal surface (per unit volume), across which the drug can be exchanged between the liposomes and the aqueous phases. The drug concentration inside the liposomal phase at position x and time t is determined by the following differential equation:

$$\frac{\partial C_{lip}(x)}{\partial t} = -\frac{3}{R_{lip}} G_D(x) \quad (17)$$

Due to size (R_{lip} approx. 200 nm) the liposomes remain immobilized in a thin layer with thickness δ (Fig. 2) at the injection site (bottom of the cuvette) for the entire duration of the experiments (24 h).

Therefore, for $X > \delta$ we have $G_D = 0$, and Eq. (16) can be written as:

$$\frac{\partial C_D}{\partial t} = D_D \frac{\partial^2 C_D}{\partial x^2} \quad (18)$$

For the cyclodextrins, the system boundary conditions require an impermeable wall at $X = X_0$ and $X = L$ (Fig. 2). Initial conditions imply i) drug absence ($C_D = 0$) for $X > \delta$ and ii) a homogeneous drug concentration distribution for $X \leq \delta$. The determination of the equilibrium concentrations implies that $G_D = 0$ and therefore:

$$G_D = \left(k_1 * C_{lip} \left(\frac{C_{DS} - C_{DE}}{C_{DS}} \right) - k_2 * C_D \left(\frac{C_{lipS} - C_{lipE}}{C_{lipS}} \right) \right) = 0 \quad (19)$$

where C_{DE} and C_{lipE} are the drug equilibrium concentrations in the aqueous and liposomal phases respectively. The solution of Eq. (19) can be performed by coupling it with the drug mass balance referring to the injected volume:

$$C_{lipE}\varphi_p + C_{DE}(1 - \varphi_p) = \frac{M_0}{V_s} = C_0 \quad (20)$$

where M_0 is the total drug amount present in the injected volume (V_s). The simultaneous solution of Eqs. (19) and (20) leads to the determination of the two unknowns: C_{DE} and C_{lipE} (see Supporting Information for more details). Time and spatial discretization of Eqs. (16–18) was performed according to the control volume method [20], while the resulting non-linear system of algebraic equations was iteratively solved by means of the Gauss-Seidel method embodying a relaxation step (relative tolerance 10^{-8}) [21] (see Supporting Information). In order to ensure stability and accuracy of the numerical solution, the time discretization step was set to 1 s while the space discretization step was set to 60 μm (1/500th of the total cuvette length). The numerical solution was achieved by means of a proper Fortran program.

3.3. Statistical analysis

Mathematical model fitting to experimental data was carried out via Excel: for each fitting, the statistical χ^2 was calculated and its value was used to perform a statistical analysis through the F-test with level of significance $\alpha = 0.05$.

4. Results and discussion

Cyclodextrins and liposomes are two different systems with respect to stoichiometry and mechanism of drug release, reflected in the similar yet slightly different mathematical approaches in the two cases, as described in the previous section. Therefore, from an experimental point of view, an important distinction in the detected diffusing species can be made. Whilst the diffusion of both free drug, cyclodextrins and drug-CD complexes influence the overall diffusion profiles, only free drug is measured in the liposomal dispersion. Once the liposomal dispersion is injected in the bottom of the cuvette (i.e. origin of the diffusion), the initial condition is a stable partition of the drug in the liposomes and free drug fraction in the aqueous media, controlled by binding (k_1) and unbinding (k_2) constants. However, few seconds after the injection, passive diffusions begins and the equilibrium is perturbed. Liposomes are large nanocarriers (min. 200 nm) with kinetics of Brownian motion orders of magnitude lower than drug molecules. Moreover, the liposomes contain a 300 mOsm/kg isotonic buffer that impedes their passive diffusion due to higher relative density in respect to the diffusion media (pure water). In this case, therefore, the only species detected by the UV laser is the free drug fraction. In order to assess the reliability of both the experimental setup and the developed mathematical model, a two-step strategy was adopted. To validate the method, the first step was to compare the numerical solution with the analytical solution of the drug diffusion profiles in absence of HP-β-CD or liposomes (i.e. only drug aqueous solution). The perfect coincidence of the two solutions proved the reliability of the numerical approach, at least in this simple situation (data not shown). Then, the developed model was fitted to the experimental data referring to drug diffusion in the cuvette (in the absence of a carrier) in order to determine the drug diffusion coefficient and to compare it with a theoretical evaluation according to the SEGWE method [26]. As the theoretical values and fitting data were very similar, this assured the validity of both the experimental and theoretical approaches. Consequentially, all measurements were performed once, supported also by our previous experience with the reproducibility of the setup [25].

4.1. Hydroxypropyl-β-cyclodextrin

Model (Eqs. (8–10)) fitting to experimental data was performed assuming as fitting parameters the total drug concentration in the injected volume (C_{D0}), the diffusion coefficients of the three diffusing species (ibuprofen: D_D; HP-β-CD: D_C; and drug-CD complex: D_{DC}) and k_1,

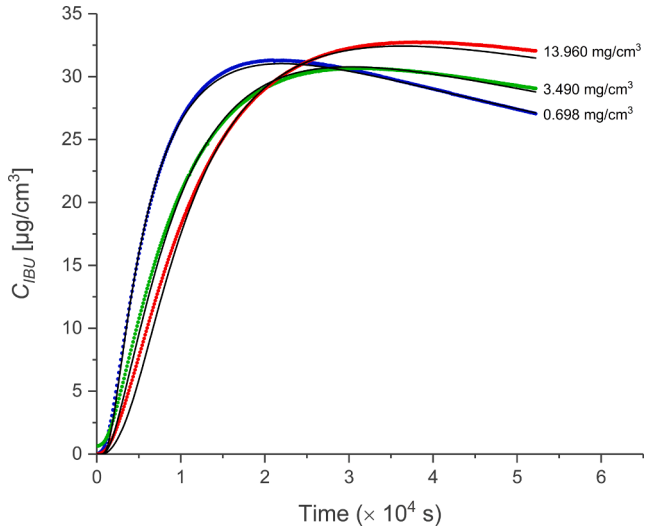

Fig. 3. Comparison between experimental data (scatter plot) and model best fitting (continuous black line) for three representative HP-β-CD concentrations (blue: 0.698 mg/cm^3; green: 3.490 mg/cm^3; red: 13.960 mg/cm^3). CIBU [µg/cm^3] indicates the total ibuprofen concentration, i.e. the sum of free and bound (to HP-β-CD) ibuprofen concentration. Note that the different amounts of cyclodextrin alter the diffusion profile of IBU. The F-test value achieved for every case corresponds to: F698 (5,433,0.95) < 89050; F1396 (5,433,0.95) < 55551; F3490 (5,433,0.95) < 27479; F6980 (5,433,0.95) < 11472; F13960 (5,433,0.95) < 20434. The subscript in the F-test values accounts for the cyclodextrin concentration of each case. (For interpretation of the references to colour in this figure legend, the reader is referred to the web version of this article.)

Table 1
Fitting parameters referring to different HP-β-CD concentrations. C_{D0} is the ibuprofen concentration in the injected volume, D_D, D_C and D_{DC} are the diffusion coefficients of the three diffusing species – ibuprofen, HP-β-CD, ibuprofen-CD complex, respectively. For simplicity, the values of the direct (k_1 = 2.26*10^{-3} [cm^3/(mg*s)]) and reverse (k_2 = 1.0*10^{-3} [s^{-1}]) kinetic constants (Eqs. (8 – 10)) were omitted from the table. The last row shows the theoretical C_{D0} value and the D_D, D_C and D_{DC} values evaluated according to the SEGWE method, assuming 0.868 mPa*s as solvent (water) viscosity at 25 °C [26].

[HP-β-CD]	C_{D0}	D_D	D_C	D_{DC}
[mg/cm^3]	[mg/cm^3]	*10^{-6} [cm^2/s]		
0.698	0.288	7.7	2.7	2.3
1.396	0.298	8.1	3.6	3.1
3.940	0.287	8.2	3.6	3.2
6.980	0.291	8.3	3.7	3.3
13.960	0.292	8.2	3.7	3.3
mean ± SD	0.291 ± 0.0043	8.1 ± 0.23	3.5 ± 0.43	3.0 ± 0.42
Reference values (calculated)	0.259	6.74*	3.05*	2.89*

while k_2 was evaluated, based on the k_1/k_2 knowledge (22.26 cm^3/µg), derived from equilibrium data [17]. Coefficients m and n were set to 1, as ibuprofen-CD stoichiometry is known to be 1:1 [7,17]. While the choice of D_D, D_C, D_{DC} and k_1 as fitting parameters is obvious, the necessity of considering also C_{D0} among fitting parameters derives from the model's high sensitivity with respect to this parameter, so that small variations in this parameter result in model output variations. As shown in Fig. 3 and as proved by the F-test (see figure caption), the agreement between model best fitting (solid black lines) and experimental data (blue, green and red scatter) is very good for all HP-β-CD concentrations considered. It should be underlined that this good agreement can be achieved only when considering the sum of the free drug (C_D) and the complexed drug (C_{DC}) as drug concentration (C_{IBU} in Fig. 3). This fact

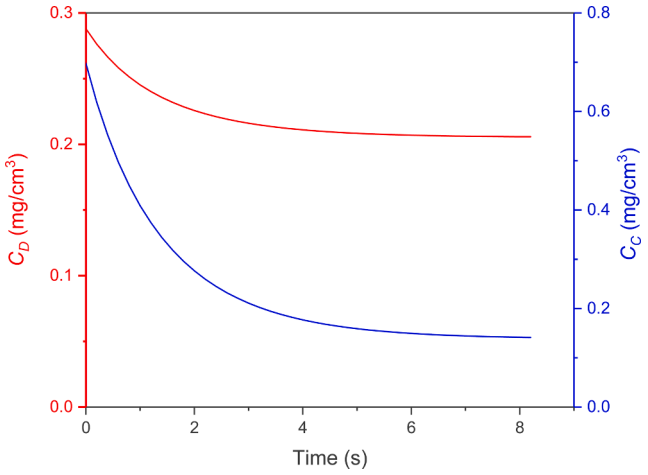

Fig. 4. Time evolution of free (not bound) ibuprofen (C_D, red line) and HP-β-CD (C_C, blue line) concentrations in the injected volume, assuming a total ibuprofen concentration (C_{D0}) of 0.288 mg/cm^3, a total HP-β-CD concentration of 0.698 mg/cm^3 and that the binding (k_1) and unbinding (k_2) constants values are those coming from model fitting to experimental data (see Table 1). (For interpretation of the references to colour in this figure legend, the reader is referred to the web version of this article.)

Table 2
Equilibrium concentrations of ibuprofen (C_D), HP-β-CD (C_C) and ibuprofen-CD complex (C_{DC}) for all the different measurements performed (values calculated according to the analytical solution (Supporting Information, Eqs. (A12–A14)) of Eqs. (12–14).

[HP-β-CD]	C_D	C_C	C_{DC}
[mg/cm^3]			
0.698	0.205	0.139	0.641
1.396	0.145	0.364	1.185
3.940	0.045	1.852	1.879
6.980	0.018	5.134	2.118
13.960	0.008	12.038	2.205

implies that HP-β-CD cannot hide the drug presence from the utilized detecting system (UV).

Another important outcome deriving from model fitting to experimental data consists in the independence of k_1 (2.26*10^{-3} (µg/(cm^3*s)) and, thus, of k_2 (10^{-4} s^{-1}) on the HP-β-CD concentration, at least in the range considered. This supports the adopted mathematical expression of the generative terms (G_D, G_C and G_{DC}; Eqs. (8–10)), which relays on the k_1 and k_2 independence on species concentration. It is also worth underlining that, as shown in Table 1, D_D, D_C and D_{DC} do not substantially vary with HP-β-CD concentration. In addition, D_D and D_C values are close to the theoretical values calculated according to the SEGWE method [26] assuming T = 25 °C and 0.868 mPa*s for what concerns liquid (water) viscosity. Finally, Table 1 reveals that also C_{D0} remains almost constant with HP-β-CD concentration and its value is close (≈ 11 % increase) to the theoretical one (0.260 mg/cm^3).

Relaying on the k_1 and k_2 values determined by data fitting (Table 1 caption), it is possible to simulate the binding and unbinding process occurring in the injectable volume once ibuprofen and HP-β-CD are incubated together. Fig. 4 reports the analytical solution of Eqs. (12–14), assuming an initial free ibuprofen concentration (C_{D0}) equal to 0.288 mg/cm^3 and an initial free HP-β-CD concentration (C_{C0}) equal to 0.698 mg/cm^3. As it can be seen, equilibrium achievement is very fast (seconds) if compared to the time elapsing between sample preparation and injection (minutes/hours). As the increase of C_{C0} makes the equilibrium attainment faster, we can conclude that in all our experiments the ibuprofen-CD interaction reached equilibrium when the solution was injected at the cuvette bottom. Thus, one important model assumption

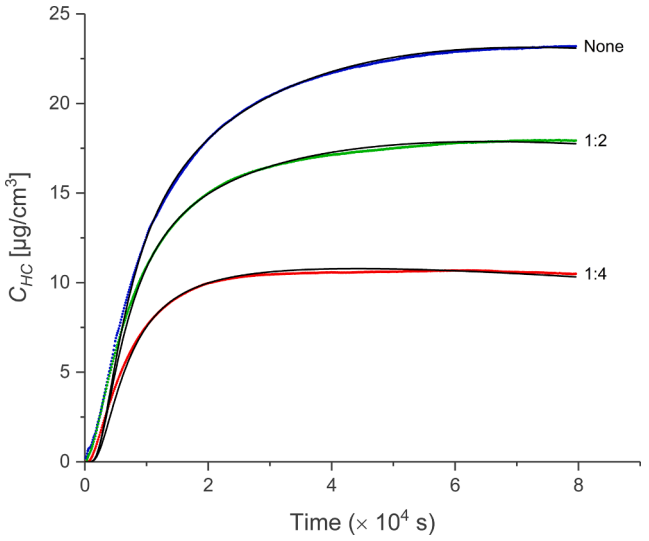

Fig. 5. Comparison between experimental data (blue: no dilution, green: dilution 1:2 and red: dilution 1:4) and model best fitting (solid black lines) referring to the three dilution conditions considered (see Table 3) in the case of pre-loaded systems. C_{HC} indicates the hydrocortisone concentration and t is time. The F-test value achieved for every case corresponds to: $F_{undiluted}$ (4,718,0.95) < 44131; $F_{1:2}$ (4,661,0.95) < 22360; $F_{1:4}$ (4,718,0.95) < 19264. The subscript in F values corresponds to the dilution in each case. (For interpretation of the references to colour in this figure legend, the reader is referred to the web version of this article.)

has been proved *a posteriori*. Table 2 sums up the equilibrium conditions occurring for the different C_{C0} values considered. Correctly, the increase in C_{C0} implies a reduction of the equilibrium free ibuprofen concentration (C_D) and an increase of the equilibrium complex (C_{DC}) concentration.

4.2. Liposomes

Model (Eqs. (18)–(20)) fitting to experimental data was performed assuming as fitting parameters the total drug concentration (C_{D0}) in the injected volume, the diffusion coefficient of the drug (hydrocortisone), D_D, and k_1, whereas k_2 was evaluated on the basis of the k_1/k_2 (=3.5) knowledge derived from equilibrium data in the limit of low drug concentration [17]. Moreover, the hydrocortisone solubility in the liposomal (C_{lipS}) and in the aqueous (C_{DS}) phases were set equal to 5.4 mg/cm^3 and 0.4 mg/cm^3 respectively [13]. C_{D0} was considered as fitting parameter due to the model high sensitivity with respect to this variable. As shown in Fig. 5 and proved by the F-test, the agreement between model best fitting (solid black lines) and experimental data (colored scatter) is very good, independently of the dilution ratio of the liposomal dispersion prior to the injection.

Remarkably, k_1 (and, thus, k_2) as well as the hydrocortisone diffusion coefficient (D_D) are practically unaltered by the dilutions (see Table 3). This fact is a proof for the correctness of the main hypothesis on which the model relies, i.e. the concentration independence of k_1, k_2 and D_D. In addition, the reliability of these results is also proved by the concordance of the determined D_D value and that coming from to the SEGWE evaluation [26], assuming T = 25 °C and fluid viscosity of 0.868 mPa*s. Interestingly, Fig. 6 shows that the developed model (eqs. (18 – 20)) can properly fit (see also F-test outcome reported in the figure caption) both loading of empty liposomes with drug (post-loaded liposomes) or drug release from loaded liposomes (pre-loaded liposomes). As the release profiles show, in the pre-loaded liposomes (blue line Fig. 6) the diffusion curve continues to rise, indicating a sustained, yet slow, release of HC from the liposomes into the aqueous media. On a contrary, in the post-loaded liposomes (Fig. 6, green line) the curve is descending (after four hours approx.) but the profile is significantly different from a drug solution. This intuitively indicates that drug is to some extent sequestered and retained by the liposomes and that partitioning equilibrium within phases is not reached yet. It is also important to underline that the resulting values of the fitting parameters k_1 and D_D are very close to those found for the systems considered in Fig. 5 (see Table 3), strengthening both the experimental and the theoretical approach developed in this paper. This ultimately means that the way liposomes are loaded with hydrocortisone does not affect the entire release kinetics process.

On the basis of the determined k_1 (and k_2) value, the developed model (Supporting Information, Eq. (A23)) allows the evaluation of the

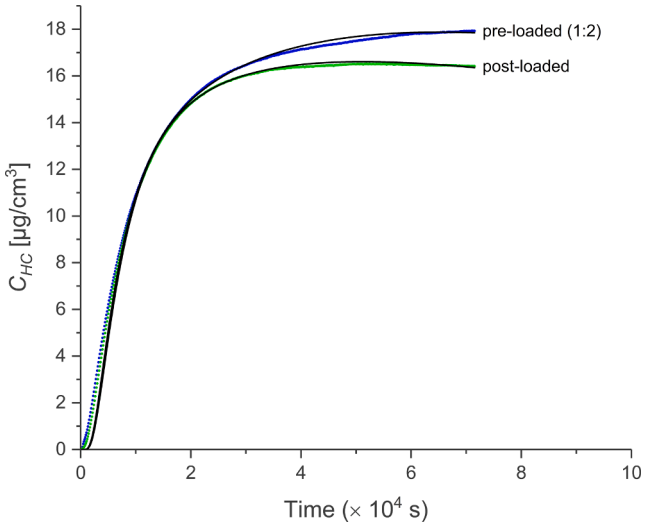

Fig. 6. Comparison between experimental data (scatter) and model best fitting (black lines) in the case of pre-loaded (dilution 1:2, blue) and post-loaded (green) liposomes systems (see Table 3). The F-test value achieved for every case corresponds to: $F_{post\text{-}loaded}$ (4,594,0.95) < 24726; $F_{1:4}$ (4,718,0.95) < 19264. The subscript in F values are useful to recognize each case. (For interpretation of the references to colour in this figure legend, the reader is referred to the web version of this article.)

Table 3
Fitting parameters referring to different dilution ratios (Fig. 5) and techniques for hydrocortisone loading inside liposomes (Fig. 6). C_{D0} is the hydrocortisone concentration in the injected volume, D_D *is* the hydrocortisone diffusion coefficient in water while k_1 and k_2 are the direct and reverse kinetic constants, respectively, (Eq. (15)) ruling hydrocortisone partitioning between the aqueous and the liposomal phases. The D_D value calculated according to the SEGWE method [26], assuming 0.868 mPa*s as solvent (water) viscosity at 25 °C is equal to 5.27 cm^2/s.

Dilution	C_{D0}		k_1	k_2	D_D	V_{lip}
	Measured (HPLC)	Calculated				
	[mg/cm^3]		10^{-10} [cm/s]		10^{-6} [cm^2/s]	10^{-3} [cm^3]
No dilution	0.430	0.293	1.70	5.95	5.25	5.20
1:2	0.215	0.225	1.60	5.60	5.42	4.65
1:4	0.110	0.125	1.70	5.95	5.42	3.20
Post-loaded	0.192	0.192	1.70	5.95	5.00	3.00

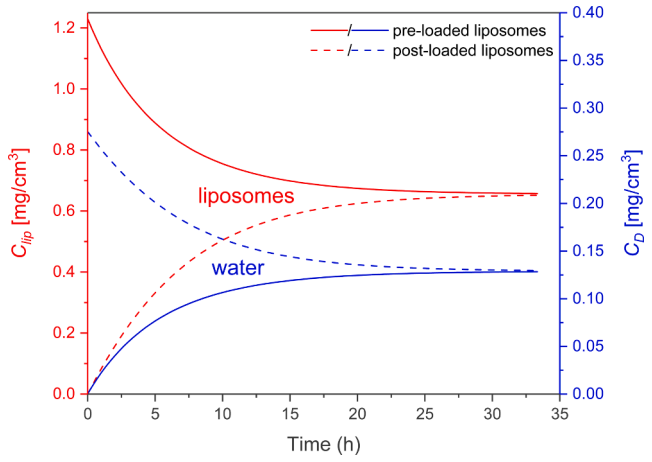

Fig. 7. Time evolution of the hydrocortisone concentration inside the liposomal (C_{lip}) and the aqueous (C_D) phases constituting the injectable volume. Dashed lines refer to the case of hydrocortisone totally confined inside the aqueous phase and absent in the liposomal phase at the beginning of drug partitioning. Solid lines refer to the case of hydrocortisone totally confined inside the liposomal phase and absent in the aqueous phase at the beginning of drug partition. Liposomes volume corresponds to that of the 1:2 dilution system of Table 3 ($4.65*10^{-3}$ cm^3) and the total hydrocortisone concentration is assumed to be 0.225 mg/cm^3.

Table 4
Hydrocortisone equilibrium concentrations in the aqueous (C_{DE}) and liposomal (C_{lipE}) phases relative to the systems considered in this paper (pre- and post-loaded liposomes). C_{D0} is the hydrocortisone concentration in the injected volume and IE is the liposomal incorporation efficiency.

Formulation	Dilution	C_{DE} [mg/cm^3]	C_{lipE}	C_{D0}	IE %
pre-loaded	none	0.152	0.842	0.293	60
	1:2	0.129	0.655	0.225	54
	1:4	0.087	0.387	0.125	40
post-loaded	none	0.130	0.661	0.192	41

time required to get the equilibrium partitioning of hydrocortisone between the aqueous phase and the liposomal one as depicted in Fig. 7. These simulations assume that the volume occupied by the liposomal phase is comparable to the 1:2 dilution system (see Table 3). Additionally, simulations were performed in two limiting conditions. In the first one (post-loaded liposomes), the drug, at the beginning of the partitioning, is completely contained in the water phase (dashed lines) and absent in the liposomal phase. In the second, on the contrary, the drug is initially totally confined in the liposomal phase and it is absent in the water phase (pre-loaded liposomes, continuous lines).

Fig. 7 shows that when the drug fills the aqueous phase and is not present in the liposomal phase (dashed lines) at the beginning of the partitioning, its concentration in the aqueous phase (dashed blue line) decreases with time while its concentration increases in the liposomal phase (dashed red line). Obviously, the opposite situation takes place when the drug is initially present only in the liposomal phase. Clearly, the equilibrium drug concentration in the aqueous (C_{DE}) and in the liposomal (C_{lipE}) phases is the same whatever the initial conditions considered. Interestingly, regardless of the initial conditions considered, the attainment of the equilibrium is reached after about 24 h, i.e. approximately to the time elapsing between formulation preparation and injection. Thus, again, the hypothesis of equilibrium attainment inside the injectable volume at injection time is confirmed also in the second carrier (liposomes) considered in this paper. Table 4 summarized all relevant fitting parameters obtained by the simulation related to liposomes.

The incorporation efficiencies (IE, Table 4) has been calculated by Eq. (21):

$$IE(\%) = \frac{(V_{lip}{*}C_{lipE})}{(C_{D0}{*}0.025)}{*}100 \quad (21)$$

Were V_{lip} and C_{lipE} are the liposomal volume and HC liposomal concentration respectively and C_{D0} is the HC concentration (Table 3) in the injected volume (0.025 cm^3). The incorporation efficiency of the original (i.e. undiluted) liposomal dispersion prepared was 60%, which is in agreement with previously reported data for such formulations [13]. Interestingly, the incorporation efficiency decreased with increasing dilution factor. As we found out, upon dilution of the suspension, hydrocortisone has a favorable exchange lipid-water. Therefore, perturbation of the equilibrium triggers concentration-gradient driven (due to k2 > k1) release of more hydrocortisone from the liposomal bilayer out in the aqueous environment. It is important to underline that hydrocortisone is a lipophilic compound therefore its loading into the phospholipid membrane of liposomes is thermodynamic favorable. Therefore, the relatively effective loading (41%) observed also in the post-loaded liposomes experiments is in accordance with expectations. All these findings are quite relevant also from a practical point of view, as all available experimental methods for incorporation efficiency determination implies perturbation of the original dispersion equilibrium (mostly dilution). For drug with a quite rapid exchange lipid-aqueous media, this might lead to overestimation of incorporation efficiency.

5. Conclusions

The presented work outlines the successful development of a simple experimental/mathematical approach for the precise determination of diffusional and kinetic parameters linked to colloidal-carrier systems (cyclodextrins and liposomes). With this cost effective and easy implementable approach, we are able to resolve drug diffusion profiles in an unstirred water layer and discriminate real time and with high accuracy, the free fraction (i.e. molecularly dissolved drug) from the bounded drug fraction to the carrier in any time point. Ultimately, for CD we calculate binding constants and for nanocarrier-based systems (liposomes in this case) we successfully measure the incorporation efficiency. As this new *in vitro/in silico* method can be easily adapted and utilized to study different types of enabling formulation in different media, we herewith are opening the gate for the solution of much more complex and biopharmaceutically relevant issues such as the optimization of *in vitro/in vivo* correlation.

Declaration of Competing Interest

The authors declare that they have no known competing financial interests or personal relationships that could have appeared to influence the work reported in this paper.

Acknowledgements

The authors would like to thank *Tove Larsen* (head engineer at the Department of Pharmacy, UiO) and *Ivar Grove* (principal engineer at the Department of Pharmacy, UiO) for their technical support and the NordForsk Grant *NordicPop (Patient Oriented Product, University Hub project #85352/D)*. Finally, author M.M.T. would like to express her gratitude to *Dr. Albena Tzankova Mihailova* for her contribution to the development of analytical methods.

Appendix

Cyclodextrins

To achieve model numerical solution, Eqs. (8)-(10) were discretized in time and space according to the implicit control volume method that allowed their transformation in a non-linear system of algebraic equations (three equations for each control volume considered). The iterative solution of the non-linear system was achieved by means of the Gauss-Seidel method embedding a relaxation step characterized by a relaxation rate of 0.65. For each control volume (i), the expression of the drug, cyclodextrin and complex concentrations were evaluated according to the following equations:

$$C_{D_i}^{t+dt} = \frac{\left(C_{D_{i+1}}^{t+dt} + C_{D_{i-1}}^{t+dt}\right)*D_D\Delta t + \Delta x^2*\left[C_{D_i}^{t} + mM_D\Delta t k_2 C_{DC_i}^{t+dt}\right]}{\Delta x^2 + 2D_D\Delta t + mM_D\Delta t\Delta x^2 k_1\left(C_{D_i}^{t+dt}\right)^{m-1}\left(C_{C_i}^{t+dt}\right)^{n}} \tag{A1}$$

$$C_{C_i}^{t+dt} = \frac{\left(C_{C_{i+1}}^{t+dt} + C_{C_{i-1}}^{t+dt}\right)*D_C\Delta t + \Delta x^2*\left[C_{C_i}^{t} + nM_C\Delta t k_2 C_{DC_i}^{t+dt}\right]}{\Delta x^2 + 2D_C\Delta t + nM_C\Delta t\Delta x^2 k_1\left(C_{D_i}^{t+dt}\right)^{m}\left(C_{C_i}^{t+dt}\right)^{n-1}} \tag{A2}$$

$$C_{DC_i}^{t+dt} = \frac{\left(C_{DC_{i+1}}^{t+dt} + C_{DC_{i-1}}^{t+dt}\right)*D_{DC}\Delta t + \Delta x^2\left[C_{DC_i}^{t} + M_{DC}\Delta t k_1\left(C_{D_i}^{t+dt}\right)^{m}\left(C_{C_i}^{t+dt}\right)^{n}\right]}{\Delta x^2 + 2D_{DC}\Delta t + M_{DC}\Delta t\Delta x^2 k_2} \tag{A3}$$

where Δx [length] is the thickness of each control volume, Δt [time] is the time discretization step, subscript i indicates the ith control volume whereas the superscript t highlights the time instant and "$t + dt$" represents the next time step. Obviously, Eqs. (A1)-(A3) expressions referring to the first and the last control volume are slightly different in order to account for the imposed boundary conditions (impermeable wall).

In order to determine of the initial values of the drug, cyclodextrin and complex concentration values in the injected volume, Eqs. (12)-(14) were numerically solved according to the Gauss-Seidel approach embedding a relaxation step characterized by a relaxation rate of 0.65. Thus, Eqs. (12)-(14) were combined to get Eqs. (A4)-(A5) in the spirit of the Gauss-Seidel approach:

$$C_{DE} = \frac{C_{D0}}{1 + \frac{M_D}{M_{DC}}*m*k*C_{DE}^{m-1}C_{CE}^{n}} \tag{A4}$$

$$C_{CE} = \frac{C_{C0}}{1 + \frac{M_C}{M_{DC}}*n*k*C_{DE}^{m}C_{CE}^{n-1}} \tag{A5}$$

where k is the ratio between the forward (k_1) and the backward (k_2) constants appearing in the definition of the generative terms G_D, G_C and G_{DC} (Eqs. (8)-(10)). In order to gain information about the speed of equilibrium attainment in the injectable volume, resorting on the expressions of G_D, G_C and G_{DC}, it is possible building up the following system of differential equations enabling the determination of the C_D, C_C and C_{DC} time evolution:

$$\frac{dC_D}{dt} = m*M_D*\left[-k_1C_D^{m}C_C^{n} + k_2C_{DC}\right] \tag{A6}$$

$$\frac{dC_C}{dt} = n*M_C*\left[-k_1C_D^{m}C_C^{n} + k_2C_{DC}\right] \tag{A7}$$

$$\frac{dC_{DC}}{dt} = M_{DC}*\left[k_1C_D^{m}C_C^{n} - k_2C_{DC}\right] \tag{A8}$$

The numerical solution of Eqs. (A6)-(A7) was achieved by their discretization according to the implicit Euler method. The resulting non-linear system of algebraic equations was solved by the Gauss-Seidel approach embedding a relaxation step characterized by a relaxation rate of 0.65:

$$C_D^{t+dt} = C_D^{t} - \frac{m*M_D*\Delta t*k_1*\left(C_D^{t+dt}\right)^{m}*\left[C_C^{t} - \frac{n*M_C}{m*M_D}*\left(C_D^{t} - C_D^{t+dt}\right)\right]^{n}}{1 + \Delta t*M_{DC}*k_2} + \frac{m*M_D*\Delta t*k_2}{1 + \Delta t*M_{DC}*k_2}C_{DC}^{t} \tag{A9}$$

$$C_C^{t+dt} = C_C^{t} - \frac{n*M_C}{m*M_D}*\left(C_D^{t} - C_D^{t+dt}\right) \tag{A10}$$

$$C_{DC}^{t+dt} = \frac{C_{DC}^{t} + M_{DC}*k_1*\left(C_D^{t+dt}\right)^{m}\left(C_C^{t+dt}\right)^{n}*\Delta t}{1 + \Delta t*M_{DC}*k_2} \tag{A11}$$

Interestingly, in the simple case of $n = m = 1$, the following analytical solution can be achieved:

$$C_D^{t+dt} = \frac{-b + \sqrt[2]{b^2 - 4ac}}{2a} \tag{A12}$$

$$a = \frac{\Delta t\,k_1M_C}{1 + \Delta t\,k_2M_{DC}}\,b = 1 + \frac{\Delta t\,k_1\left(M_DC_C^{t} - M_CC_D^{t}\right)}{1 + \Delta t\,k_2M_{DC}} \tag{A13}$$

$$c = -\left(C_D^{t} + C_{DC}^{t}\frac{M_D\,\Delta t\,k_2}{1 + \Delta t\,k_2M_{DC}}\right) \tag{14)}$$

Liposomes

Combining Eqs. (15) and (16), we get:

$$\frac{\partial C_D}{\partial t} = \left(\frac{1-\varphi_s}{1-\varphi_p}\right) * D_D \frac{\partial^2 C_D}{\partial x^2} + \frac{3}{R_{lip}} * \left(\frac{\varphi_p}{1-\varphi_p}\right) * \left[k_1 C_{lip}\left(\frac{C_{DS}-C_D}{C_{DS}}\right) - k_2 C_D\left(\frac{C_{lipS}-C_{lip}}{C_{lipS}}\right)\right] \tag{A15}$$

While Eq. (A15) holds inside the injected volume (X ≤ δ), elsewhere in the cuvette (X > δ), Eq. (17) holds as liposomes always reside in cuvette bottom (X ≤ δ). In order to get the spatial and time variation of drug concentration, both equations have to be numerically solved. Their discretization in space and time according to the control volume method allows getting a non-linear system of algebraic equation (one for each control volume) that is iteratively solved by the Gauss-Seidel approach embedding a relaxation step characterized by a relaxation rate of 0.65:

$$C_{D_i}^{t+dt} = \frac{\left(\frac{1-\varphi_s}{1-\varphi_p}\right)\frac{D_D \Delta t}{\Delta x^2}\left[C_{D_{i+1}}^{t+dt} + C_{D_{i-1}}^{t+dt}\right] + C_{D_i}^{t} + \frac{3\Delta t k_1}{R_{lip}}\left(\frac{\varphi_p}{1-\varphi_p}\right) C_{lip_i}^{t+dt}}{\left[1 + \frac{2D_D\Delta t}{\Delta x^2}\left(\frac{1-\varphi_s}{1-\varphi_p}\right) + \frac{3\Delta t}{R_{lip}}\left(\frac{\varphi_p}{1-\varphi_p}\right)\left(k_1 \frac{C_{lip_i}^{t+dt}}{C_{DS}} + k_2 \frac{C_{lipS} - C_{lip_i}^{t+dt}}{C_{lipS}}\right)\right]} X \le \delta \tag{A16}$$

$$C_{D_i}^{t+dt} = \frac{\frac{D_D \Delta t}{\Delta x^2}\left[C_{D_{i+1}}^{t+dt} + C_{D_{i-1}}^{t+dt}\right] + C_{D_i}^{t}}{\left[1 + \frac{2D_D\Delta t}{\Delta x^2}\right]} X > \delta \tag{A17}$$

Obviously, Eq. (A16) expression referring to the first control volume is slightly different in order to account for the imposed boundary condition, i.e. impermeable wall in X = 0. Similarly, eq. (A17) expression referring to the last control volume is slightly different in order to account for the imposed boundary condition, i.e. impermeable wall in $X = L$. Finally, the expression of the first control volume occurring for X > δ differs from eq. (A17) as it embodies the condition of equal fluxes in $X = \delta$, i.e. the drug flux leaving the cuvette portion filled by liposomes (X ≤ δ) must be equal to the drug flux entering the cuvette portion without liposomes.

Eq. (17) derives from the local drug mass balance performed in X:

$$V_{lip}\frac{\partial C_{lip}(x)}{\partial t} = -N_{lip} * 4\pi R_{lip}^2 G_D(x) \tag{A18}$$

where V_{lip} and N_{lip} represent, respectively, the volume and the number of liposomes contained between "X" and "X + ΔX" while R_{lip} is the average liposomes radius. Remembering that:

$$V_{lip} = N_{lip} * \frac{4}{3}\pi R_{lip}^3 \tag{A19}$$

Eq. (A18) becomes Eq. (17). Its solution in each one of the control volumes occurring for X ≤ δ allows to get $C_{lip}(X)$. Also in this case, Eq. (17) discretization was performed according to the implicit Euler method. In the light of the Gauss Seidel approach, Eq. (17) can be written as:

$$C_{lip_i}^{t+dt} = \frac{C_{lip}^{t} + \frac{3\Delta t}{R_{lip}} k_2 C_{D_i}^{t+dt}}{1 + \frac{3\Delta t}{R_{lip}}\left[\left(\frac{k_2}{C_{lipS}} - \frac{k_1}{C_{DS}}\right) C_{D_i}^{t+dt} + k_1\right]} X \le \delta \tag{A20}$$

In order to evaluate the equilibrium drug concentrations in the aqueous (C_{DE}) and liposomal (C_{lipE}) phases forming the injectable volume, eqs. (19) and (20) have to be simultaneously solved. After some algebraic manipulations, we get:

$$C_{DE} = \frac{-B \pm \sqrt[2]{B^2 - 4AC}}{2A} \quad C_{lipE} = \frac{C_0 - C_{DE}(1-\varphi_p)}{\varphi_p} \tag{A21}$$

$$A = \frac{C_{lipS}}{C_{DS}} - \frac{k_2}{k_1} \quad B = C_{lipS}\left(1 + \frac{\varphi_p}{1-\varphi_p}\frac{k_2}{k_1}\right) + \frac{C_0}{1-\varphi_p} \quad A\,C = \frac{C_0 C_{lipS}}{1-\varphi_p} \tag{A22}$$

The positive root of Eq. (A21) has to be considered.

In order to gain information about the speed of equilibrium attainment in the injectable volume, resorting on G_D expression (Eq. (15)), it is possible building up the following system of equations enabling the determination of the C_{DE} and C_{lipE} time evolution:

$$\frac{dC_{lip}}{dt} = -\frac{3}{R_{lip}}\left[k_1 C_{lip}\left(\frac{C_{DS}-C_D}{C_{DS}}\right) - k_2 C_D\left(\frac{C_{lipS}-C_{lip}}{C_{lipS}}\right)\right] \tag{A23}$$

$$C_D = \frac{C_0 - C_{lip} * \varphi_p}{1-\varphi_p} \tag{24)}$$

Eq. (A23) is a differential kinetics equation ruling the drug exchange between the liposomal and aqueous phases, while Eq. (A24) represents the drug mass balance performed on the injectable volume. Upon Eq. (A23) discretization according to the implicit Euler method and after some rearrangements, we get:

$$C_{lip}^{t+dt} = \frac{-\alpha \pm \sqrt[2]{\beta^2 - 4\alpha\gamma}}{2\alpha} \quad C_D^{t+dt} = \frac{C_0 - C_{lip}^{t+dt} * \varphi_p}{1-\varphi_p} \tag{A25}$$

where:

$$\alpha = \left[\frac{3\Delta t * \varphi_p}{R_{lip}} * \left(\frac{k_2}{C_{lipS}} - \frac{k_1}{C_{DS}}\right)\right] \tag{A26}$$

$$\beta = \left[-\left(\left(1-\varphi_p\right) + \frac{3\Delta t}{R_{lip}} \left(k_2\varphi_p + \frac{k_2 C_0}{C_{lipS}} + k_1\left(1-\varphi_p\right) + \frac{k_1 C_0}{C_{DS}} \right) \right) \right] \tag{A27}$$

$$\gamma = C_{lip}^{t} * \left(1-\varphi_p\right) + \frac{3\Delta t}{R_{lip}} k_2 C_0 \tag{A28}$$

The positive root of Eq. (A25) has to be considered.

References

[1] V.P. Torchilin, Recent advances with liposomes as pharmaceutical carriers, Nat. Rev. Drug. Discov. 4 (2005) 145–160, https://doi.org/10.1038/nrd1632.

[2] U. Bulbake, et al., Liposomal Formulations in Clinical Use: An Updated Review, Pharmaceutics 9 (2017) 12, https://doi.org/10.3390/pharmaceutics9020012.

[3] T. Loftsson, M.E. Brewster, Pharmaceutical Applications of Cyclodextrins. 1. Drug Solubilization and Stabilization, J. Pharm. Sci. 85 (1996) 1017–1025, https://doi.org/10.1021/js950534b.

[4] European Medicines Agency. *Background review for cyclodextrins used as excipients (EMA/CHMP/333892/2013)*. 2014 [cited 2022 May]; Available from: https://www.ema.europa.eu/en/documents/report/background-review-cyclodextrins-used-excipients-context-revision-guideline-excipients-label-package_en.pdf.

[5] *Veklury, Summary of Product Characteristics*. 2021 [cited 2022 May]; Available from: https://www.ema.europa.eu/en/documents/product-information/veklury-epar-product-information_en.pdf.

[6] M. di Cagno, et al., Liposomal solubilization of new 3-hydroxy-quinolinone derivatives with promising anticancer activity: a screening method to identify maximum incorporation capacity, J. Liposome Res. 21 (2011) 272–278, https://doi.org/10.3109/08982104.2010.550265.

[7] M.P. di Cagno, The Potential of Cyclodextrins as Novel Active Pharmaceutical Ingredients: A Short Overview, Molecules 22 (2016) 1, https://doi.org/10.3390/molecules22010001.

[8] K. Sugano, K. Terada, Rate- and Extent-Limiting Factors of Oral Drug Absorption: Theory and Applications, J. Pharm. Sci. 104 (2015) 2777–2788, https://doi.org/10.1002/jps.24391.

[9] R.L. Carrier, L.A. Miller, I. Ahmed, The utility of cyclodextrins for enhancing oral bioavailability, J. Control. Release 123 (2007) 78–99, https://doi.org/10.1016/j.jconrel.2007.07.018.

[10] T. Loftsson, et al., Effects of cyclodextrins on drug delivery through biological membranes, J. Pharm. Sci. 96 (2007) 2532–2546, https://doi.org/10.1002/jps.20992.

[11] M.F. Peralta, et al., Liposomes can both enhance or reduce drugs penetration through the skin, Sci. Rep. 8 (1) (2018) 13253–13311, https://doi.org/10.1038/s41598-018-31693-y.

[12] A. Dahan, J.M. Miller, The Solubility-Permeability Interplay and Its Implications in Formulation Design and Development for Poorly Soluble Drugs, AAPS J. 14 (2012) 244–251, https://doi.org/10.1208/s12248-012-9337-6.

[13] M. di Cagno, B. Luppi, Drug "supersaturation" states induced by polymeric micelles and liposomes: A mechanistic investigation into permeability enhancements, Eur. J. Pharm. Sci. 48 (2013) 775–780, https://doi.org/10.1016/j.ejps.2013.01.006.

[14] Lin, M. and X.-R. Qi, *Purification* Method of Drug-Loaded Liposome, in: W.-L. Lu and X.-R. Qi (Eds.), Liposome-Based Drug Delivery Systems, Springer Berlin Heidelberg:,Berlin, Heidelberg, 2018, p. 1-11.DOI: 10.1007/978-3-662-49231-4_24-1.

[15] F.L. Holzem, et al., Microdialysis and nanofiltration allow to distinguish molecularly dissolved from colloid-associated drug concentrations during biomimetic dissolution testing of supersaturating formulations, Eur. J. Pharm. Sci. 174 (2022) (2022), 106166, https://doi.org/10.1016/j.ejps.2022.106166.

[16] M.P. di Cagno, et al., Experimental Determination of Drug Diffusion Coefficients in Unstirred Aqueous Environments by Temporally Resolved Concentration Measurements, Mol. Pharm. 15 (2018) 1488–1494, https://doi.org/10.1021/acs.molpharmaceut.7b01053.

[17] M.P. di Cagno, P.C. Stein, Studying the effect of solubilizing agents on drug diffusion through the unstirred water layer (UWL) by localized spectroscopy, Eur. J. Pharm. Biopharm. 139 (2019) 205–212, https://doi.org/10.1016/j.ejpb.2019.04.005.

[18] A. Samad, Y. Sultana, M. Aqil, Liposomal Drug Delivery Systems: An Update Review, Curr. Drug Deliv. 4 (2007) 297–305, https://doi.org/10.2174/156720107782151269.

[19] M. Grassi, et al., Understanding drug relaease and absorption mechanisms : a physical and mathematical approach, CRC Press, Boca Ration, Fla, 2007.

[20] S.V. Patankar, Numerical heat transfer and fluid flow. Series in computational methods in mechanics and thermal sciences, Hemisphere Publ, Washington, 1980.

[21] S.C. Chapra, R.P. Canale, Numerical Methods for Engineers with Programming and Software Applications, New York, WCB/McGraw-Hill, 1998, p. 288.

[22] M. Grassi, N. Coceani, L. Magarotto, Modelling partitioning of sparingly soluble drugs in a two-phase liquid system, Int. J. Pharm. 239 (2002) 157–169, https://doi.org/10.1016/S0378-5173(02)00101-1.

[23] J.T.M. Van De Waterbeemd, et al., Transport in QSAR IV: The interfacial drug transfer model. Relationships between partition coefficients and rate constants of drug partitioning, Pharm. Weekbl. 3 (1981) 224–237.

[24] M. Abrami, et al., Antibacterial drug release from a biphasic gel system: Mathematical modelling, Int. J. Pharm. 559 (2019) 373–381, https://doi.org/10.1016/j.ijpharm.2019.01.055.

[25] M.M. Tzanova, et al., Towards a better mechanistic comprehension of drug permeation and absorption: Introducing the diffusion-partitioning interplay, Int J. Pharm. 608 (2021) 9, https://doi.org/10.1016/j.ijpharm.2021.121116.

[26] R. Evans, et al., Improving the Interpretation of Small Molecule Diffusion Coefficients, Anal. Chem. 90 (2018) 3987–3994, https://doi.org/10.1021/acs.analchem.7b05032.